J Sol-Gel Sci Technol (2015) 75:323–335
DOI 10.1007/s10971-015-3703-7

ORIGINAL PAPER

Preparation and characterization of in situ entrapment of laccase in silica microparticles via an ambient drying procedure

Azmi Fadziyana Mansor[1] · Nur Atikah Mohidem[1] · Wan Nurul Izyani Wan Mohd Zawawi[1] · Nurul Sakinah Othman[1] · Salasiah Endud[2] · Hanapi Mat[1,2]

Received: 19 January 2015 / Accepted: 1 April 2015 / Published online: 14 April 2015

Abstract A simple and reproducible method for in situ entrapment of laccase in silica microparticles was studied which involved hydrolysis and condensation of tetraethyl orthosilicate via sol–gel route using one-step (base catalyst) and two-step (acid–base catalyst) methods followed by an ambient drying procedure. The influence of method used, starting material compositions, and aging conditions toward polymeric structure and catalytic activity of the laccase entrapped silica microparticles (LSMs) were investigated. It was found that one-step method is not suitable for in situ entrapment purpose since it left significant amount of untrapped laccase in the reaction media and lead to laccase inactivation due to its active site alteration by continuous contact with basic condition. Conversely, the laccase was entirely entrapped in the silica matrices synthesized using the two-step method with the highest specific activity of 434.71 U/g obtained for the immobilized laccase. In addition, the LSM showed stability improvement toward pH and temperature compared to the free laccase and was able to retain more than 80 % of their initial catalytic activity after 1 month of storage duration. The treatment of the LSM with trimethylchlorosilane resulted in the increase in the surface hydrophobic properties which is expected to be useful for applications in non-aqueous medium.

Graphical Abstract

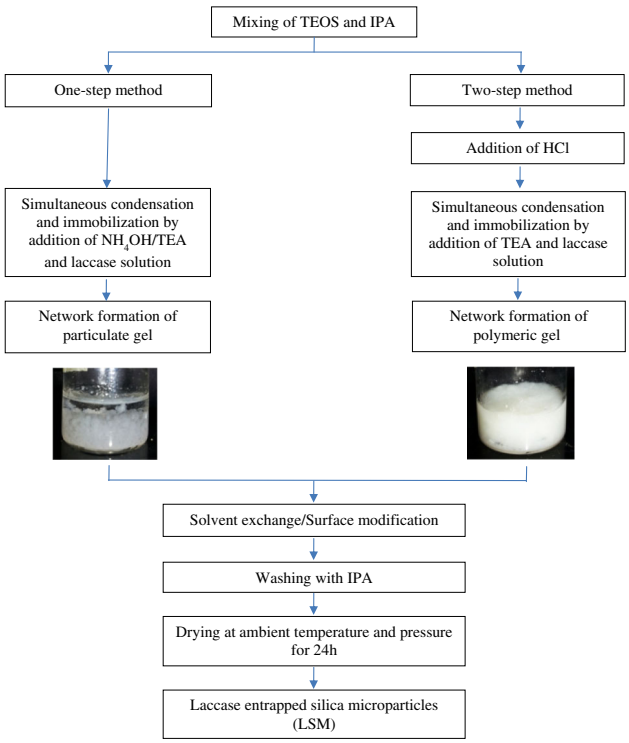

Keywords Silica microparticles · Entrapment · Laccase · Catalytic activity

1 Introduction

Silica materials have become a common choice when selecting immobilization supports for biocatalysts. Their inert properties, which are chemically stable over a broad pH

✉ Hanapi Mat
hbmat@cheme.utm.my

[1] Advanced Materials and Process Engineering Laboratory, Faculty of Chemical Engineering, Universiti Teknologi Malaysia (UTM), 81310 Skudai, Johor, Malaysia

[2] Novel Materials Research Group, Nanotechnology Research Alliance, Universiti Teknologi Malaysia (UTM), 81310 Skudai, Johor, Malaysia

and temperature range, stand out among other available support materials. Moreover, the synthesis conditions can be manipulated to produce various types of silica materials such as silica gels (e.g., xerogel, cryogel, and aerogel) and mesoporous silicas (e.g., SBA, HMM, and MCM) to suit their application as the biocatalyst support matrices. In addition, the end products such as particle size, pore diameter, structural ordering of the pores, as well as thermal and mechanical stability can be easily tailored by manipulating the synthesis conditions and the drying procedures. Therefore, it should be pointed out that the flexibility of the synthesis conditions has become the main advantage for silica materials to be selected as the support materials for enzyme immobilization not only for biocatalytic applications, but also for biosensing, biofuels, and enzyme-controlled drug delivery system [1].

Generally, silica gels are prepared via sol–gel polymerization of silicon alkoxides. The process mainly involves the hydrolysis of the alkoxide group and subsequent condensation reaction of the silanol groups to produce siloxane bonds and the by-products (i.e., alcohol and water). They can exist in xerogel or cryogel form by evaporation and freeze dry technique, which cause rupture to the 3D networks and lead to the formation of dense particles. Or else, it exists as an aerogel which is obtained via solvent exchange by replacing the liquid content in the wet gel with air through supercritical or subcritical procedures. Mesoporous silicas, on the other hand, are another variation of the typical silica gels. The formation of mesoporous materials involves an addition of surfactant as a templating agent in the sol–gel synthesis. The 3D networks will be formed around the self-assembled template which will later be removed by calcination or extraction, resulting in mesoporous materials.

The applications of the silica materials such as silica gel, silica aerogel, and mesoporous silicas have been reported for enzyme immobilization by either ex situ or in situ strategies [1]. The ex situ immobilization involves either adsorption or covalent binding between enzyme and silica support surfaces. It requires the silica materials with amino-functionalized materials to be prepared using APTES and ABTMS as precursors to provide alkylamine moieties on the silica surfaces. The NH_2-modified silica supports were further functionalized with reactive aldehyde groups to act as anchoring sites for the enzyme. The enzyme attachment was performed by forming a bridging molecular unit between the silica support and the enzyme through reaction between –CHO groups in the silica material with an amino group from the enzyme in solution. For instances, Wang et al. [2] demonstrated the adsorption of laccase on mesoporous molecular sieve MCM-41 which retained 40 % of residual activity after 10 cycles and improved its thermal, pH, and operational stability. A similar positive result for laccase immobilization was reported by Liu et al. [3] using silanized and GLU-activated silica nanoparticles as a support. The thermal and operational stabilities of laccase were improved, demonstrated by the retention of 61 % of the residual activity after 4 h at 60 °C and the retention of 55 % of the activity after 10 cycles of operation.

The in situ technique involves, on the other hand, the immobilization of enzyme either by entrapment or by encapsulation method during the synthesis of the support materials [4, 5]. It offers a controlled of enzyme loading and also is expected to be less time-consuming and thus could lead to a preparation cost reduction. Santalla et al. [6] reported that encapsulation of HRP in mesoporous silica materials had worked successfully since enzyme was kept "alive" and it stayed confined selectively inside the mesoporous cages. In situ immobilization of laccase in sol–gel silica was also able to maintain their catalytic activity after 70 days of storage at room temperature [5]. This result indicates that both ex situ and in situ immobilization techniques result in the greater operational stability and durability of the immobilized laccase. However, the ex situ procedure becomes disadvantageous since the process is somehow time-consuming and often results in lower immobilization yield as well [7, 8].

Besides the immobilization strategies, the structure and morphology can also affect both the enzyme loading and the catalytic activity. Compared with enzyme immobilized on monolithic supports, microparticle or nanoparticle supports could achieve a much higher enzyme loading capacity which significantly enhanced mass transfer efficiency by the high surface-to-volume ratio. The presence of matrix in monolith form can restrain the large proteins to move through the nanopores of the hydrogel network [9]. Fan et al. [10] suggested that smaller particles will decrease the enzyme diffusion distance and minimize empty space far down the pores. Furthermore, shorter pores may give an improved availability of the enzyme toward the substrate where the substrate may be able to reach a larger relative amount of active sites within a certain time. These characteristics highlight the advantages of having the support matrix in particulate form. Even though the enzyme immobilization and development of immobilized laccase have been recently reviewed [1, 11], studies concerning in situ immobilization of enzymes in silica materials having particulate morphology are occasionally reported.

We demonstrated herein a simple and reproducible method for in situ preparation of laccase entrapped silica microparticles (LSMs) via ambient drying procedure which offer greater surface area than the one in monolith form. The ambient drying procedure provides an added advantage since it does not require any equipment or harsh conditions that could inactivate the entrapped laccase. On

these bases, we synthesized laccase entrapment in silica microparticles by two methods: (a) one-step (base catalyst) and two-step (acid–base catalyst) carried out at various starting material compositions and aging conditions. The synthesized products were characterized in terms of their pH stability, thermal stability, and storage duration. Subsequently, the influence of method used, starting material compositions, and aging conditions toward polymeric structure and catalytic activity were also investigated.

2 Materials and methods

2.1 Materials

Analytical grade reagents from various suppliers were used without further purification. 2,2-Azino-bis(3-ethylbenzothiazoline-6-sulfonate) sodium salt (ABTS), acetonitrile, sodium acetate, and n-hexane were purchased from Sigma-Aldrich (USA). 2,6-Dimethoxyphenol (2,6-DMP), ammonia solution (NH_4OH), triethylamine (TEA), isopropanol (IPA), trimethylchlorosilane (TMCS), and tetraethyl orthosilicate (TEOS) were purchased from Merck (Germany). Laccase from *T. versicolor* was purchased from Daiwa Kasei Co. Ltd. (Japan). The purity of the laccase powder was 30 % (w/w) of pure protein and 70 % (w/w) of dextrin, having molecular weight of 62 kDa and the pI of 3. The reagent water type 1 produced by the Purite Water System model Select Analyst HP40 (UK) was used in solution preparation, while the double-distilled water was used for glassware cleaning.

2.2 Experimental procedures

2.2.1 In situ entrapment procedure

The laccase entrapped in silica microparticles was synthesized by one-step and two-step methods as simplified in the Fig. 1. Generally, the synthesis involves three major steps: (1) the preparation of the alcogel by either one-step or two-step methods of sol–gel process, (2) entrapment of laccase through condensation of silicon alkoxide, and (3) the ambient drying of the wet gel to remove the trapped solvent from the pores of the gel. The one-step method was carried out using base catalyst either NH_4OH or TEA, starting material comprising of TEOS: IPA: NH_4OH (1:38.8:3.6 by molar ratio), and 1 ml of laccase solution which were mixed simultaneously and stirred at a constant speed of 500 rpm for 2 h. The laccase solution having concentration of 5 mg/ml was prepared using 0.4 M and pH 7 phosphate buffer. Table 1 shows the detailed compositions of the starting materials for the one-step method. In two-step method, the sol was first partially hydrolyzed under acidic condition using 0.05 M HCl solution in first step with stirring at constant speed of 500 rpm for 2 h before an addition of laccase solution and TEA in the second step. The detailed compositions of the starting materials are given in Table 2. The resultant alcogels from both syntheses were aged for 1 h to strengthen the gel network and then preceded with solvent exchange using solvent comprising of silane: isopropanol: hexane solution (1:1:2 by molar ratio) for 2 h. The silane was changed from TEOS to TMCS in the solvent for surface modification. The sample was then washed with IPA, and the laccase concentration in wash solution was determined by using the Biuret method [12]. The mass of laccase entrapped in the silica matrices was determined by mass balance. The wet sample was dried at room temperature (30 °C) and then stored in an airtight Teflon bottle at 5 °C. This sample was designated as laccase entrapped silica microparticles coded as either 1-LSM (one-step method) or 2-LSM (two-step method).

In order to determine the leaching potential of the LSM, the accurate weight of the LSM was placed in the 10 ml, 0.4 M, and pH 7 phosphate buffer solution, stirring for 30 min using a magnetic stirrer at 500 rpm. The leached laccase in the phosphate buffer solution was determined by using the Biuret method.

2.2.2 Catalytic activity assay

The catalytic activity of free laccase and LSM was determined by using ABTS ($\varepsilon_{436} = 29{,}300\ M^{-1}\ cm^{-1}$) as a substrate according to Leonowicz et al. [13]. The reaction medium consisted of 1 mM ABTS in 100 mM, pH 5 sodium acetate buffer; 0.05 g of sample was placed into a reaction medium, and the change in absorbance at 436 nm was recorded up to 5 min using UV/VIS spectrophotometer model PerkinElmer LAMBDA 35 (USA). The catalytic activity of laccase was calculated using Eq. 1 derived from the Beer–Lambert law;

$$\text{Catalytic activity}, A(U) = \frac{10^6 \Delta A}{\varepsilon \Delta t} \quad (1)$$

where ΔA is the increase in absorbance at 436 nm, ε is the molar absorption coefficient ($M^{-1}cm^{-1}$), Δt is the reaction time in minute, and $\Delta A/\Delta t$ is the slope of the absorbance versus time. One unit of catalytic activity A (U) is defined as the amount of enzyme that released 1 μmole per minute of oxidized product, whereas the specific activity A_s (U/g) is obtained by dividing the catalytic activity with actual mass of the laccase present in the sample.

2.2.3 Stability assessment

Stability assessment of the free laccase and LSM toward pH, thermal, and storage duration was studied. The effect

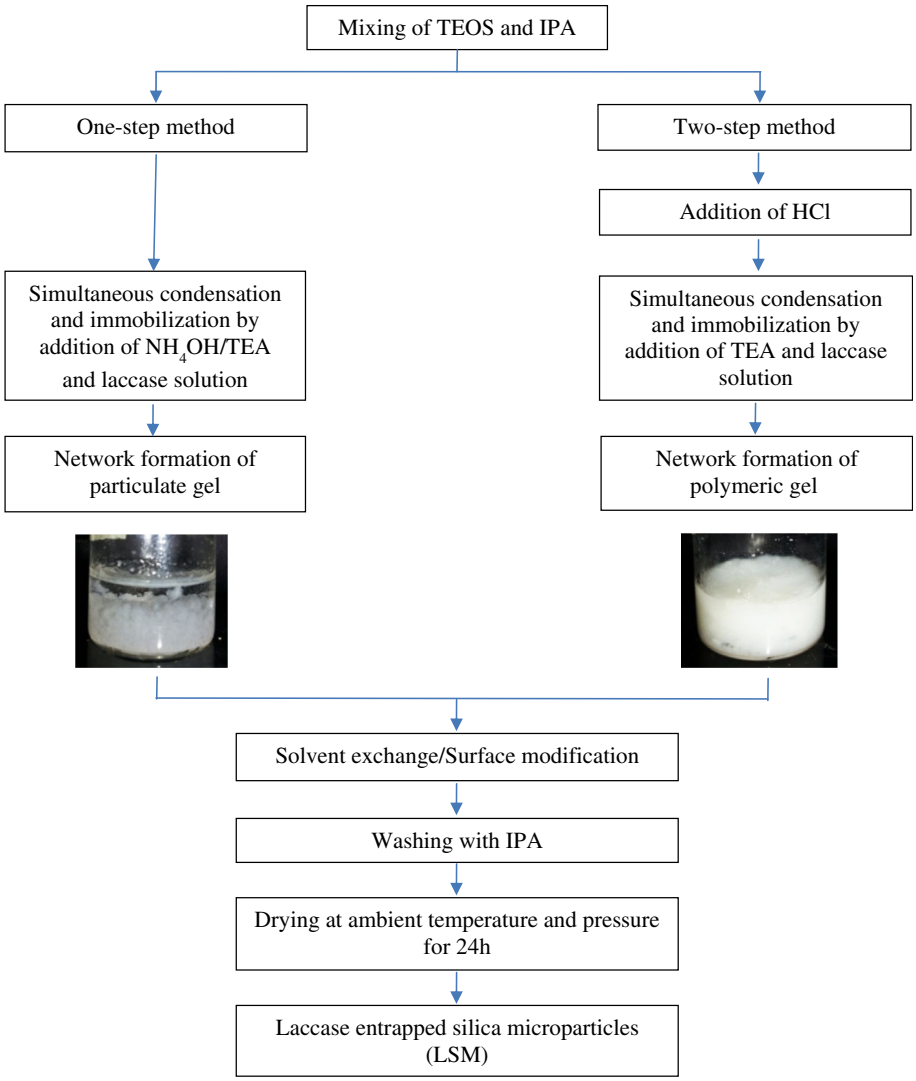

Fig. 1 Schematic representation of LSM synthesis

Table 1 Detail composition of the starting material for the one-step method

Synthesis parameters	Sample code	TEOS:IPA (v/v)	NH_4OH (mol × 10^3)	TEA (mol × 10^3)	Laccase loading (mg/ml)
Types of catalysts	1-LSM1	0.05	18.00	–	1.50
	1-LSM2	0.05	25.00	–	1.50
	1-LSM3	0.05	–	18.00	1.50
	1-LSM4	0.05	–	25.00	1.50

of the pH on the enzyme stability was studied by varying the pH of the substrate solution. As for thermal stability, the sample was exposed to different temperatures (40, 50, 60, 70, and 80 °C) for 1 h prior to analysis. The stability against storage duration was also investigated for 30 days of storage duration at room temperature (30 ± 1 °C). The catalytic activity was determined by the previously described procedure, and the results obtained were compared to the free laccase.

2.2.4 Sample characterization

A JSM-6390LV (JEOL, USA) scanning electron microscope (SEM) was used to examine the surface morphology of silica microparticles. The sample was sputter-coated with a thin layer of gold to avoid electrostatic charging during the examination with an accelerating voltage of 10–15 kV. The microstructure of the sample was carried out by transmission electron microscopy (TEM) Tecnai G2

Table 2 Detail composition of the starting material for the two-step method

Synthesis parameters	Sample code	TEOS:H_2O (v/v)	IPA (mol × 10^3)	HCl (mol × 10^6)	TEA (mol × 10^3)	Laccase loading (mg/ml)	Specific activity (U/g)
TEOS:H_2O ratios	2-LSM1	**0.80**	1.30	5.00	0.72	1.50	8.48
	2-LSM2	1.60	1.30	5.00	0.72	1.50	171.59
	2-LSM3	**2.50**	1.30	**5.00**	**0.72**	1.50	213.01
	2-LSM4	4.20	1.30	5.00	0.72	1.50	162.32
	2-LSM5	5.80	1.30	5.00	0.72	1.50	0.54
HCl	2-LSM6	2.50	1.30	0.25	0.72	1.50	14.64
	2-LSM7	2.50	1.30	0.50	0.72	1.50	183.44
	2-LSM8	2.50	1.30	**1.50**	0.72	1.50	297.75
	2-LSM9	2.50	1.30	12.50	0.72	1.50	190.19
TEA	2-LSM10	2.50	1.30	5.00	0.22	1.50	10.58
	2-LSM11	2.50	1.30	5.00	**1.80**	1.50	26.41
	2-LSM12	2.50	1.30	5.00	3.60	1.50	108.86
Laccase loading	2-LSM13	2.50	1.30	5.00	0.72	1.50	138.70
	2-LSM14	2.50	1.30	5.00	0.72	3.00	309.83
	2-LSM15	2.50	1.30	5.00	0.72	6.00	434.71
	2-LSM16	2.50	1.30	5.00	0.72	15.00	244.81

* Samples with bold have SEM images presented in Fig. 3 as starting material composition comparison

200 kV (Fei, USA). The specific surface area of the sample was measured by the nitrogen adsorption–desorption technique carried out at a temperature of 77 K, and the pore size distribution was calculated on the basis of desorption branch of the isotherm plot by Barret–Joyner–Halenda (BJH) analysis using a Micromeritics ASAP 2020 (USA) accelerated surface area and porosity analyzer. Different types of functional groups in the sample were identified by using the Fourier transform infrared (FTIR) spectrophotometer model Nicolet IS5 (Thermo Fisher Scientific, USA) equipped with attenuated total reflectance (ATR) sampling technique. A small amount of sample was placed on top of the sample holder of ATR which was made from ZnSe crystal. The related functional groups present in the absorbents were further identified using OMNIC operating system (version 7.0, Thermo Nicolet). The experiment was carried out over spectral range, varying from 4000 to 500 cm^{-1}.

3 Results and discussion

3.1 Effect of preparation methods

The laccase entrapped silica microparticles (LSMs) were prepared through the sol–gel process using TEOS as a silica precursor. In this process, the sol (or solution) evolves gradually toward the formation of a gel-like network containing both liquid and solid phases. The formation of the silica gels involves the reaction of a silicon alkoxide with water in a solvent in the presence of basic and/or acidic catalyst. The TEOS serves as the source of silicon alkoxide which reacts with water to form silanol (Si–OH) groups. These silanol groups can then react either with each other or an alkoxide group (Si–OR) to form a siloxane bridge (Si–O–Si), resulting in the joining of two molecules into one larger molecule. The molecule interconnected to form a polymer of continuous network which later condensed in a gel form. The sol–gel routes for silica gel formation using TEOS as a precursor generally consist of hydrolysis, polymerization, and condensation reactions (Eqs. 2–4).

$$\mathrm{Si\ (OC_2H_5)_4 + 4H_2O \rightarrow Si\ (OH)_4 + 4C_2H_5OH} \quad (2)$$

$$\mathrm{Si\ (OH)_4 + (OH)_4Si \rightarrow (OH)_3Si - O - Si\ (OH)_3 + H_2O} \quad (3)$$

$$\mathrm{Si\ (OH)_4 + (OC_2H_5)_4Si \rightarrow (OH)_3Si - O - (OC_2H_5)_3 + C_2H_5OH} \quad (4)$$

These reactions depend on the catalyst used which can be carried out either by one-step or two-step methods. It was observed that the silica gel prepared by the one-step method was settled down after reaction completed and left unreacted medium as depicted in Fig. 1. Contrarily, the formation of silica gel by polymerization of the entire reaction medium was observed by the two-step method. The difference in the silica gel formation was studied in order to

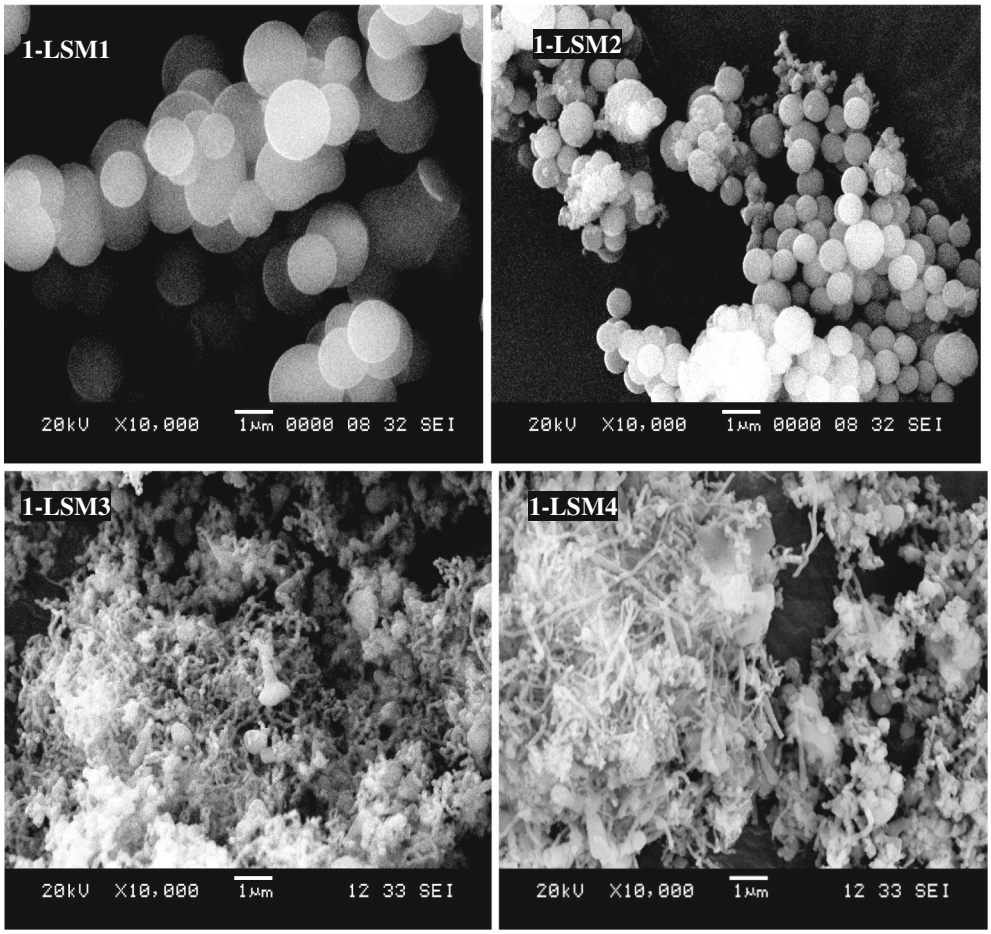

Fig. 2 SEM images of LSM synthesized via one-step method

discover their suitability for in situ enzyme immobilization. In one-step method, the base catalyst either an ammonia solution which is the most applied base catalyst or TEA from alkylamine group was used. The reaction media will turn turbid after the catalyst was added as a result of the particles formation. A huge number of primary particles is nucleated and rapidly aggregated to form stable particles [14]. Since the condensation is faster than hydrolysis in the base catalyst synthesis, polymerization produced silica gels in particulate form [15]. According to Stöber et al. [16], the size of silica particles decreases with increasing concentration of the base catalyst since both the rate of hydrolysis and condensation become faster. The difference in particle size can be observed from 1-LSM1 and 1-LSM2 with increasing NH_4OH concentration (Fig. 2). The use of TEA as a catalyst resulted in an irregular particle shape and agglomerated to a rod-like form, and the size is much smaller than NH_4OH as a catalyst as depicted by 1-LSM3 and 1-LSM4 (Fig. 2). These differences indicate the different roles that NH_4OH and TEA solutions play in the silica formation process. The ammonia solution solely functions as the catalyst where the primary particles grow up either by monomer addition or by aggregation mechanism forming well-defined silica microspheres. On the other hand, the TEA acts not only as a catalyst but it also influences the growth of the primary particles by their assembler with silica species [17]. Reducing the amount of TEA used did not change the morphology, only it became less dense. The most important point is that none of the above conditions are suitable for in situ entrapment of laccase in silica matrices. Even though the condensation takes place rapidly once the catalyst was added, it still left a significant amount of untrapped laccase in the reaction medium and continuous contact with basic condition has altered the active site of laccase. As a result, no activity was detected from the entrapped laccase. Thus, it is concluded that one-step method using base catalyst is not suitable for in situ entrapment of laccase due to the alteration of the active sites of the laccase by the reaction medium.

As for the two-step method, the LSM synthesis was carried out by a combination of acid catalyst (HCl solution) followed by a base catalyst (TEA solution). With acid catalyst, the hydrolysis kinetics is faster than the

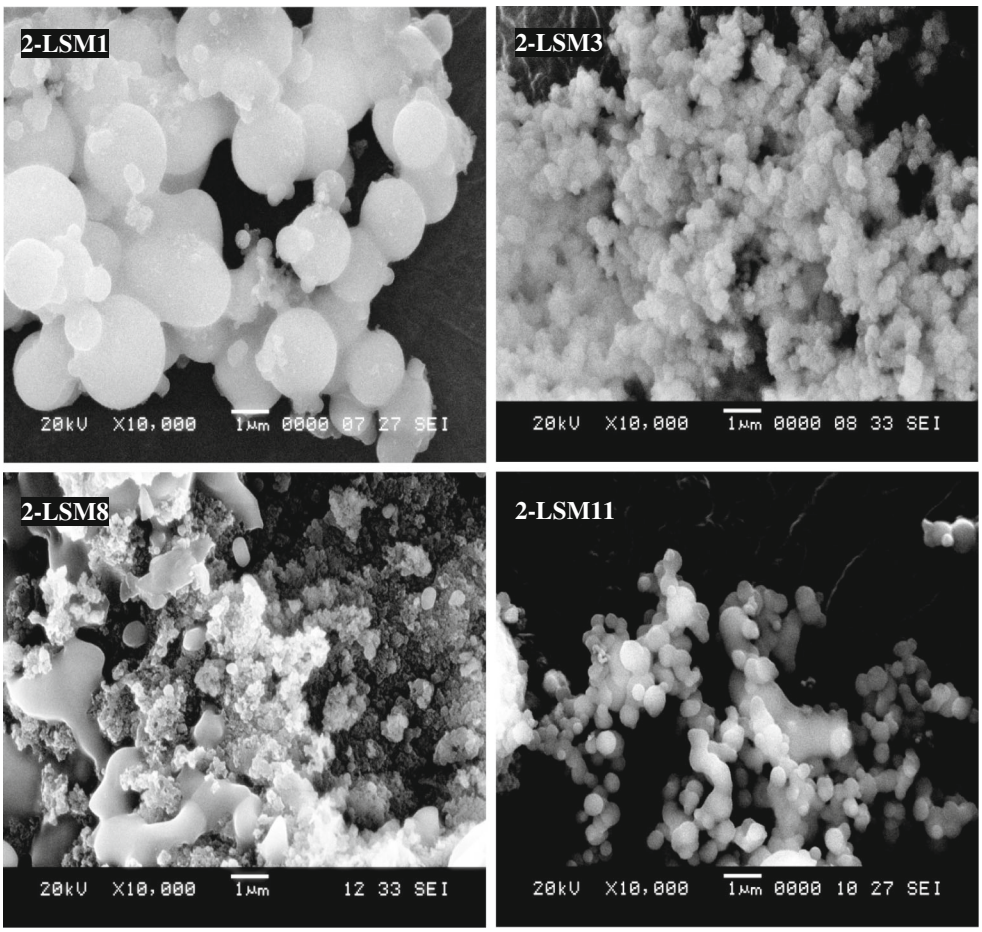

Fig. 3 SEM images of starting material composition synthesized by two-step method

condensation yielding polymeric gel having entangled linear or randomly branched chains consisting of sub-colloidal chemical units. The acid-catalyzed hydrolysis and condensation lead to generally a weakly branched and microporous structure. For that reason, a combination with base catalyst is favorable in order to decrease the microporosity and promotes a broader distribution of larger pores in silica gels [18]. The base catalyst (TEA) acts as a gelating agent as well as to accelerate the condensation process and reduce the gelation time. The formation of the particulate and polymerized gel is manipulated for in situ immobilization of laccase. The laccase solution was introduced into the reaction media right before the addition of the TEA. As a consequence, a rapid condensation minimized the contact time between the laccase and the surrounding environment. The laccase was retained in the silica matrices where leaching is unlikely to occur and protected without alteration on the laccase native structure. As a result, the entrapped laccase from a two-step method using an acid–base catalyst (HCl/TEA) was able to retain its activity compared to one-step method using either NH_4OH or TEA solution; however, it depends on the synthesis conditions used such as TEOS/water ratios, catalyst concentrations, and laccase loadings.

3.2 Effect of starting material compositions

Figure 3 compares the SEM images of samples prepared using a two-step method with different starting material compositions. The effect of TEOS compositions on morphology is given by 2-LSM1 and 2-LSM3. The decrease in TEOS concentration has reduced the rate of hydrolysis which results in the formation of larger agglomerate sphere-like polymeric framework as well as bigger pore size. The occurrence of such pore size will be useful to overcome mass transfer limitation; however, if the pores are too big, it might cause enzyme leakage and lower the retention capability. The SEM images indicate that the increase in acid concentration resulted in denser silica formation as indicated by 2-LSM3 and 2-LSM8. The dense matrix can be explained by the formation of smaller pores that exert high capillary pressure on the gel network during drying leading to the collapse of the gel network. As for the base catalyst, higher TEA concentration as depicted by

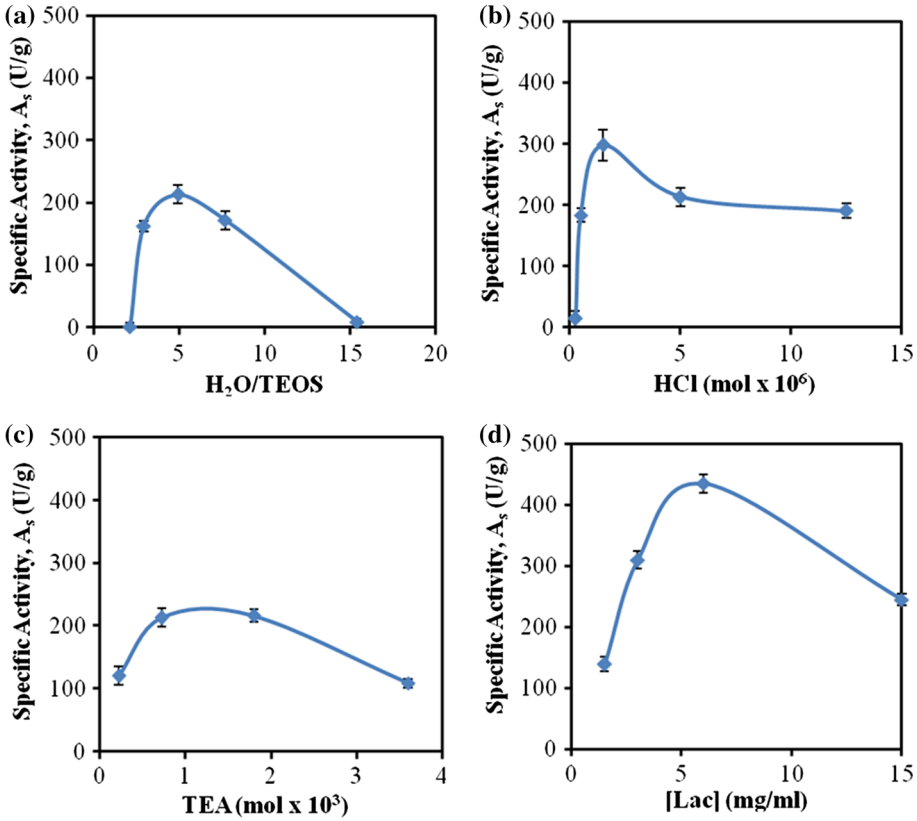

Fig. 4 Effect of starting material compositions: **a** TEOS; **b** HCl; **c** TEA; and **d** laccase loading on the specific activity of the LSM

2-LSM3 and 2-LSM11 in Fig. 3 resulted in the spherical shape becoming more irregular due to the assemblage of TEA as previously discussed.

The starting material compositions also influence the catalytic activity as depicted in Fig. 4. In Fig. 4a, the higher catalytic activity was demonstrated by H_2O/TEOS compositions of between 3 and 8, and it decreased with composition outside that range. As for the HCl concentrations, the highest catalytic activity was achieved at 1.5×10^{-6} mol HCl as shown in Fig. 4b. The catalytic activity decreased tremendously for HCl lower than that, and from experimental observation, the condensation will consume longer time after addition of TEA. The exposure of laccase to the reaction medium during the condensation process possibly altered the active sites of the laccase which explained the decrease in the laccase catalytic activity. The same situation went with the lower and higher TEA concentrations as depicted in Fig. 4c. In the former case, the amount of TEA was not enough to condense the whole reaction media, and for the latter case, the excess amount of TEA was introduced to the media. These results indicate that the starting material compositions have their effects toward morphological structure and catalytic activity of the LSM. However, specific interactions between the structure and catalytic activity remain uncertain.

3.3 Effect of enzyme loading

The difference between the specific catalytic activity of the immobilized and free enzyme in the solution is normally used to measure the immobilization efficiency. The catalytic activity of the immobilized enzymes inside the support material is often different compared to that of the free enzymes. Zhou and Hartmann [19] concluded that there is a gap of knowledge in the understanding of how the microenvironment and material properties of the mesoporous particles affect the activity of the immobilized enzymes. Hence, both positive and negative patterns have been demonstrated for the correlation between specific activity and enzyme loading [20].

Figure 4d shows the effect of laccase loading during immobilization toward catalytic activity. The concentration of laccase used was based on the actual laccase amount with purity of 30 % (w/w) of the laccase powder. The result shows that the catalytic activity was highly influenced by the increment of laccase loading from 1.5 to 6 mg/ml; however, the value was slowly decreased afterward. It is suggested that the decrease in catalytic activity derives from the steric hindrance by the excess amount of entrapped laccase and oversaturation of the pore space in the silica matrices [21]. A similar pattern for enzyme loading was also reported by Mohidem and Mat [22].

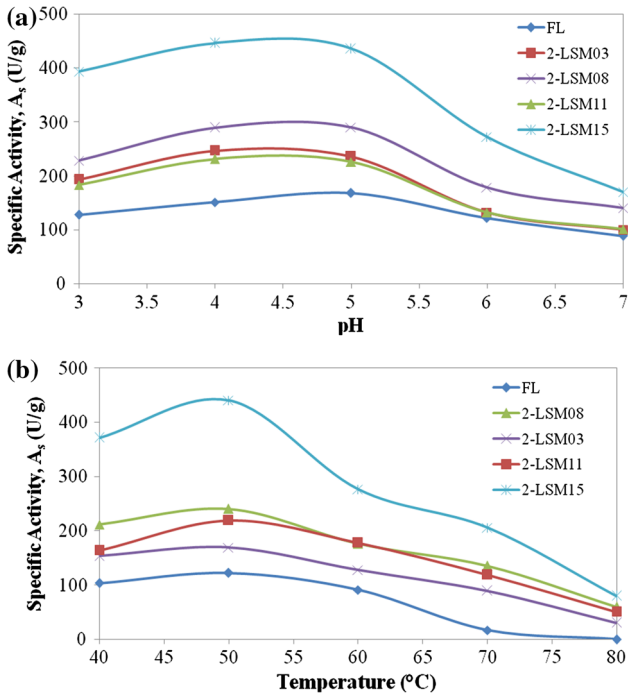

Fig. 5 Effect of **a** pH and **b** temperature on the specific activity of free laccase and LSM

3.4 Aging conditions

In the entrapment process, the laccase was simultaneously entrapped into silica polymer matrices formed via sol–gel reactions of silicon alkoxides. Such harsh condition with high temperature and pressures is not favorable for in situ laccase entrapment. An alternative drying process via ambient drying procedure was therefore used. The main procedures adopted for ambient pressure drying include network strengthening and solvent exchange/surface modification of hydrogel via silylation to avoid shrinkage or cracking during drying [23]. In this study, isopropanol (IPA) and hexane were used as solvents for exchanging with the pore liquids. An addition of TEOS to the solvent was mainly to strengthen the polymeric framework as well as to support incomplete hydrolysis. The surface hydroxyl groups are responsible for the hydrophilic nature of the silica surfaces. For the surface modification study, the TMCS was added instead of TEOS to the solvent. The existence of methyl groups results in dehydroxylation of the silica surfaces leading to increased surface hydrophobicity in which the OH groups were replaced by $(CH_3)_3$ groups. The surface area of the hydrophobic LSM increased up to 394.51 m^2/g. In addition, this hydrophobic LSM floats on the water surface, and thus, the catalytic activity cannot be determined by using the reaction mixture of ABTS solution. The catalytic activity of the hydrophobic LSM was confirmed qualitatively by reacting with 2,6-DMP in acetonitrile in which the LSM particles turned yellowish color as the product formed remained in the hydrophobic LSM as a result thus complicating the determination of the catalytic activity of the entrapped laccase. This hydrophobic LSM offers advantages for laccase oxidation and other applications in nonaqueous medium.

The effect of aging time was also investigated. Vega and Scherer [24] demonstrated that the condensation of silica gels continues long after gelation due to the large

Table 3 Effect of storage duration on the specific activity of entrapped laccase

Synthesis parameters	Sample code	Day 0 (U/g)	Day 4 (U/g)	Day 10 (U/g)	Day 30 (U/g)	Residual activity (%)
TEOS:H_2O	2-LSM1	8.48	8.45	8.09	5.44	64.15
	2-LSM2	171.59	171.50	162.24	152.89	89.10
	2-LSM3	213.01	212.95	200.17	180.36	84.67
	2-LSM4	162.32	162.32	155.66	127.79	78.73
	2-LSM5	0.54	0.55	0.51	0.32	58.89
HCl	2-LSM6	14.64	14.58	13.95	12.78	87.32
	2-LSM7	183.44	183.41	173.51	154.95	84.47
	2-LSM8	297.75	297.61	279.75	250.88	84.26
	2-LSM9	190.19	190.25	182.45	166.30	87.44
TEA	2-LSM10	120.58	120.44	116.59	111.75	92.68
	2-LSM11	216.41	216.40	207.74	191.00	88.26
	2-LSM12	108.86	108.90	104.44	97.69	89.74
Laccase loading	2-LSM13	138.70	139.02	130.68	127.59	91.99
	2-LSM14	309.83	310.00	293.26	283.09	91.37
	2-LSM15	434.71	434.55	405.44	390.41	89.81
	2-LSM16	244.81	244.78	230.09	218.15	89.11

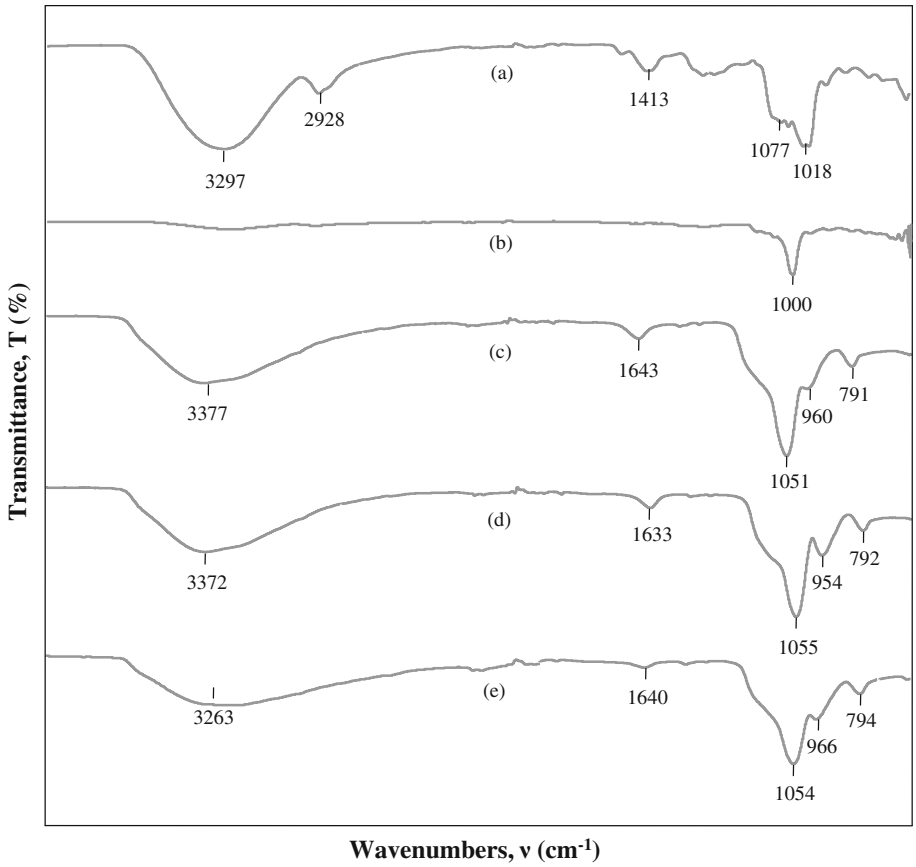

Fig. 6 FTIR spectra of *a* free laccase, *b* denatured free laccase, *c* hydrophilic LSM, *d* hydrophobic LSM, and *e* denatured LSM samples

concentration of labile hydroxyl groups. By creating new bonds bridging separate chains, the later polymerization reaction helps to stiffen and strengthen the polymeric network which consequently helps to reduce network rupture during drying process that may lead to a dense particles and smaller pore sizes. In this study, aging time was set only for 2 h since further aging time has decreased the catalytic activity of the entrap8ped laccase. The aging solution might change the pH in the silica gel and cause the dissolution of silica which later affects the entrapped laccase.

3.5 Stability assessment

The effect of pH on the catalytic activity of the free laccase and LSM was investigated at different pH values varying from 3 to 7 (Fig. 5a). The free laccase shows lower activity compared to the LSM which might be due to a direct contact between laccase and the surrounding environment and consequently affects their stability. As for the LSM, all samples show the same pattern where the maximum specific activity is slightly shifted to more acidic region and their stability decreased as pH increased. The ionization potential of the phenolic compounds weakened as the pH increases due to the formation of the phenolate anion. This condition does not, however, apply to ABTS and other substrates which are electron donors because protons are not involved in the oxidation of such substrates. Since the influence of pH on redox potential is insignificant, the gradually decreased catalytic activity as depicted in Fig. 5a is more likely related to the binding of hydroxide ion at the *T*2/*T*3 site of laccase which altered the active site compositions [25].

The effect of the temperature on the catalytic activity of free laccase and LSM was determined in the range of 40–80 °C (Fig. 5b). It could also be observed that the specific activity of the free laccase and LSM was strongly dependent on temperature, and both were gradually decreased as the temperature increased. The specific activity of free laccase experienced a sudden fall at 70 °C and completely inactivated at the higher temperature of 80 °C. However, in comparison with the free laccase, the LSM exhibits remarkable catalytic stability and a broader temperature profile. The higher stability of the LSM was probably due to the restricted conformational mobility of the molecules after immobilization which kept the laccase from injuring due to direct exposure to environment changes. Such accomplishment was assisted by the nature of silica support that is completely inert and stable at elevated temperatures.

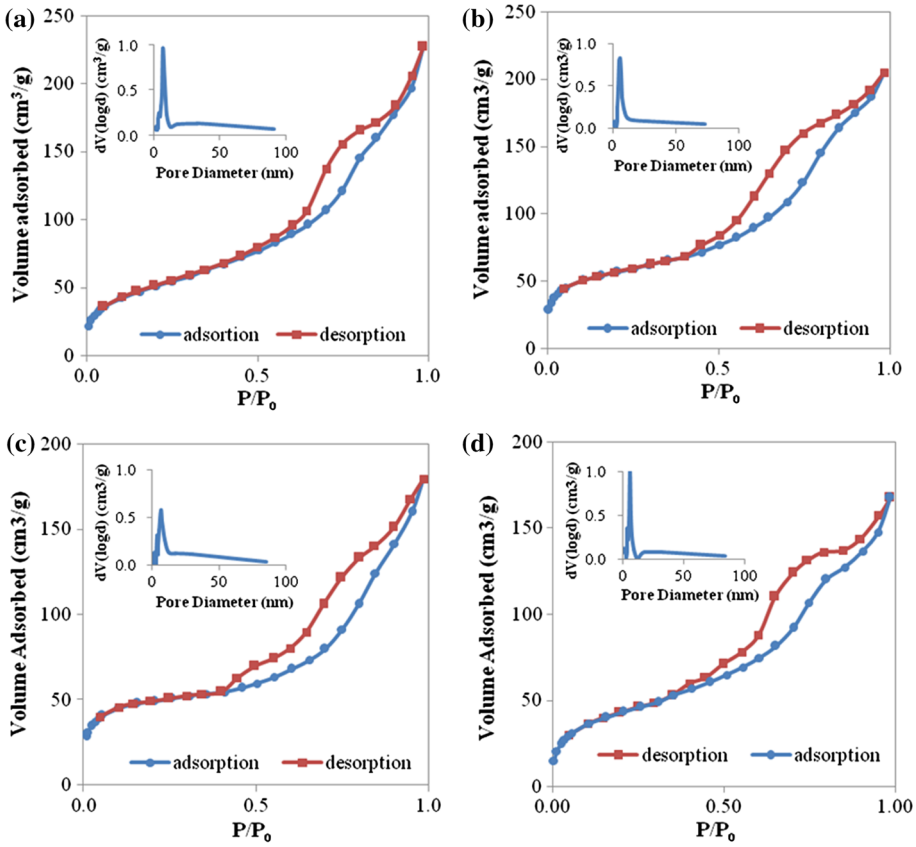

Fig. 7 Nitrogen adsorption/desorption isotherm and pore size distribution of **a** 2-LSM3, **b** 2-LSM8, **c** 2-LSM11, and **d** 2-LSM15

Table 4 Textural properties of 2-LSM3, 2-LSM8, 2-LSM 11, and 2-LSM15

Sample code	Surface area, A_s (m^2/g)	Pore volume, V_p (cm^3/g)	Pore diameter, D_p (nm)
2-LSM3	228.16	0.36	6.52
2-LSM8	199.08	0.30	4.94
2-LSM11	167.06	0.27	1.42
2-LSM15	214.02	0.27	5.61

Another stability assessment apart from the pH and temperature is the storage duration. The storage stability of the entrapped laccase at 27 °C for 30 days is stated in Table 3. The result shows that most of the LSMs are able to maintain 80–90 % of the initial specific activity after 1 month. These results indicate that the LSMs have shown stability improvement through immobilization as compared to the free laccase which has completely denatured afterward.

3.6 Structural and spectroscopic analysis of LSM

Figure 6 shows the FTIR spectra of the free laccase, denatured free laccase, hydrophilic LSM, hydrophobic LSM, and denatured LSM. The FTIR spectrum for the free laccase shows a visible spike in the NH_2 stretching region observed at 3900–3400 cm^{-1} that comes from the amino groups of the protein molecules. However, this band was significantly missing as the protein denatured (Fig. 6b). The C–O bond for laccase is represented by the peaks at 1018 and 1077 cm^{-1}. As for the LSM, the large and broad band at 3200–3500 cm^{-1} is the characteristics of the OH stretching bonds. For both free and LSM spectra, the stretching vibration of –OH is from the silanol groups (Si–OH) and some adsorbed water molecules. In general, this strong peak is related to the hydrolysis and polycondensation of TEOS which leads to the existence of hydroxyl groups on the surface of silica matrices. Thus, the increase in the peak intensity observed for the LSM spectra may be due to the overlapping of those peaks originally from silica matrices and laccase. On the other hand, the band became broader and slightly less intense for the LSM sample as the immobilized laccase denatured and reduced its catalytic activity throughout the stability assessment period. The previous band is usually accompanied by another absorption peak at 1600 cm^{-1} which belongs to the –OH

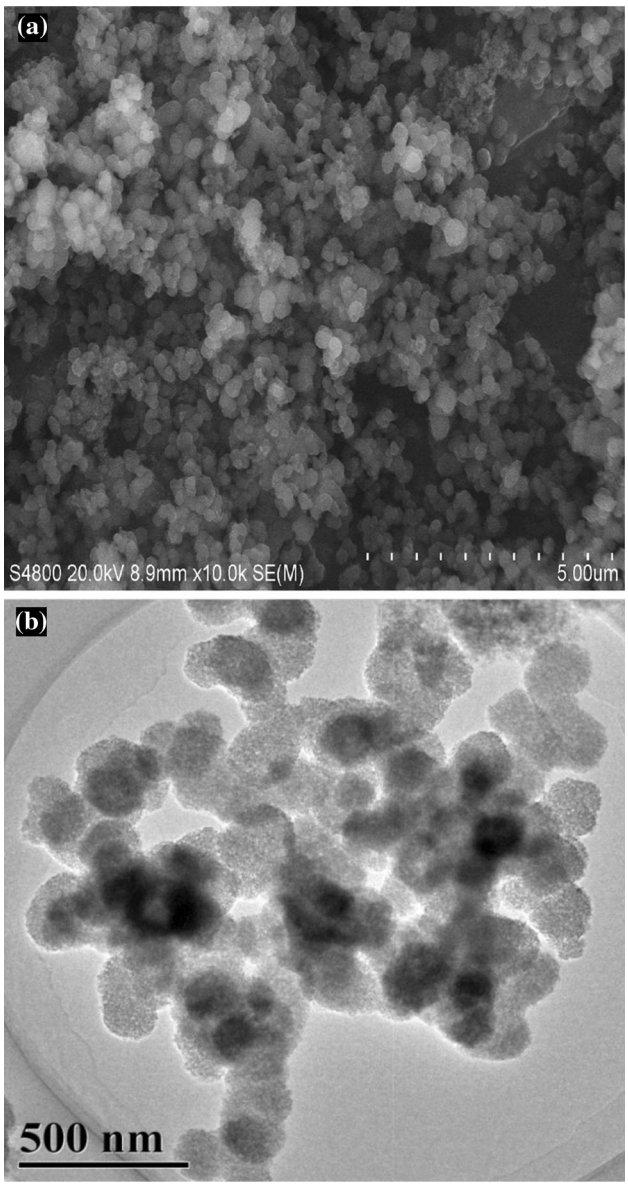

Fig. 8 **a** SEM and **b** TEM images of 2-LSM15

vibrations of adsorbed water [26]. The existence of silica matrices is clearly illustrated by the internal asymmetric stretching of Si–O–Si bonds at 900 and 1100 cm^{-1}. The 2-LSM15 which represents the hydrophilic LSM was compared with the hydrophobic LSM obtained after undergoing surface modification of the hydrophilic LSM (i.e., 2-LSM15) using TMCS during solvent exchange process. The surface chemical modification can be confirmed from the FTIR spectrum of the hydrophobic LSM given in Fig. 6d with another visible spike detected at 954 cm^{-1} attributed to the Si–C stretching bonds.

The textural properties of the selected LSM samples were further compared by examining their nitrogen adsorption–desorption isotherms and pore size distributions. A large accessible surface area between 157.61 and 205.98 $m^2\ g^{-1}$ of type IV isotherm was observed. The H_1-type hysteresis loop of type IV isotherm is typical for mesoporous materials. The pore size distribution with a pronounced peak in the mesopore region (2–50 nm) is depicted in Fig. 7. It shows that the preparation through a two-step method was able to produce silica support with mesoporous characteristics. Nonetheless, there were still slight changes in the textural properties due to the variation of the starting material compositions (Table 4). The changes in starting material compositions generally would affect the particle size and morphology of the silica structures. Thus, it would lead to differences in surface area, pore volume, and pore diameter. Table 4 shows that even though the 2-LSM15 holds the best catalytic activity, the total pore volume is the lowest compared to other samples. The decrease in total pore volume was attributed to the higher amount of laccase present in the 2-LSM15, which may have created extra bonding with silica matrix forming larger particle size, thus decreasing the total pore volume.

As shown previously in Table 2, the 2-LSM15 gives the highest catalytic activity over other synthesized 2-LSM samples. Therefore, the physicochemical characteristics of the 2-LSM15 were analyzed for further understanding. The microscopic appearance (Fig. 8a) shows a 3D skeleton of silica microstructures built from interconnected spheres with uniform shape and size of around 1 μm. The interconnected network of the 2-LSM15 was exhibited by a highly porous structure with various pore sizes as depicted in the TEM image (Fig. 8b). Besides, the orderly shaped morphology would eventually provide a better contact between immobilized laccase and the available substrate.

4 Conclusions

The laccase from *T. versicolor* was successfully entrapped in silica microparticles (LSMs) prepared by a two-step acid–base method and an ambient drying procedure. The one-step method was found to be unsuitable for the laccase immobilization in silica matrices. The specific activity of the LSM depends on the starting materials composition, types, and concentrations of the catalyst and laccase loading with the highest specific activity obtained for the 2-LSM15 (434.71 U/g). The LSMs show stability improvement toward pH and temperature profile and are also able to maintain 80–90 % of the initial specific activity after 1 month storage duration.

Acknowledgments Financial supports of the Research University Grant (GUP Grant No. 06H85) from UTM, the Fundamental Research Grant Scheme (FRGS Grant No. 4F218) form MOHE, and eScience

Research Grant (eScience Grant No. 4S071) from MOSTI are gratefully acknowledged.

References

1. Fernández-Fernández M, Sanromán MÁ, Moldes D (2012) Biotechnol Adv 31:1808–1825
2. Wang Y, Zheng X, Zhao M (2008) J Chem Eng Chin Univ 22:83–87
3. Liu Y, Guo C, Wang F, Liu C, Liu H (2008) Chin J Process Eng 8:583–588
4. Dai Y, Niu J, Liu J, Yin L, Xu J (2010) Bioresour Technol 101:8942–8947
5. Mohidem NA, Mat HB (2012) J Sol–Gel Sci Technol 61:96–103
6. Santalla E, Serra E, Mayoral A, Losada J, Blanco RM, Diaz I (2003) Solid State Sci 13:691–697
7. Huang J, Xiao H, Li B, Wang J, Jiang D (2006) Biotechnol Appl Biochem 44:93–100
8. Huang J, Liu C, Xiao H, Wang J, Jiang D, Gu E (2007) Int J Nanomedicine 2:775–784
9. Sakai-Kato K, Kato M, Toyo'oka T (2002) Anal Chem 74:2943–2949
10. Fan J, Lei J, Wang L, Yu C, Tu B, Zhao D (2003) Chem Commun 7:2140–2141
11. Carlsson N, Gustafsson H, Thörn C, Olsson L, Holmberg K, Åkerman B (2014) Adv Colloid Interface Sci 205:339–360
12. Ohnishi ST, Barr JK (1978) Anal Biochem 86:193–200
13. Leonowicz A, Sarkar JM, Bollag J-M (1988) Appl Microbiol Biotechnol 29:129–135
14. Bogush GH, Zukoski CF (1991) J Colloid Interface Sci 142:19–34
15. Dorcheh AS, Abbasi MH (2008) J Mater Process Technol 199:10–26
16. Stöber W, Fink A, Bohn E (1968) J Colloid Interface Sci 26:62–69
17. Zhao H, Xin Y, Wang H, Zhang Z, Liu S (2011) J Inorg Organomet Polym 21:925–928
18. Rao AV, Rao AP, Kulkarni MM (2004) J Non-Cryst Solids 350:224–229
19. Zhou Z, Hartmann M (2012) Top Catal 55:1081–1100
20. Lei CH, Shin Y, Magnuson JK, Fryxell G, Lasure LL, Elliott DC (2006) Nanotechnology 17:5531–5538
21. Lei Z, Jiang Q (2011) J Agric Food Chem 59:2592–2599
22. Mohidem NA, Mat HB (2009) J Appl Sci 9:3141–3145
23. Rao AV, Nilsen E, Einarsrud MA (2001) J Non-Cryst Solids 296(3):165–171
24. Vega AJ, Scherer GW (1989) J Non-Cryst Solids 111:153–166
25. Morozova V, Shumakovich GP, Gorbacheva MA, Shleev SV, Yaropolov AI (2007) Biochem-Mosc 72:1136–1150
26. Shen J, Zhang Z, Wu G, Zhou B, Ni X, Wang J (2006) J Mater Sci Technol 22:798–802